Natural Products Targeting the Fungal Unfolded Protein Response as an Alternative Crop Protection Strategy

Thomas Charpentier, Guillaume Viault, Anne-Marie Le Ray, Nelly Bataillé-Simoneau, Jean-Jacques Helesbeux, Nadège Blon, Franck Bastide, Muriel Marchi, Sophie Aligon, Antoine Bruguière, et al.

Natural products targeting the fungal Unfolded Protein Response as an alternative crop protection strategy.

Thomas Charpentier[a,b], Guillaume Viault[a], Anne-Marie Le Ray[a], Nelly Bataillé-Simoneau[b], Jean-Jacques Helesbeux[a], Nadège Blon[a], Franck Bastide[b], Muriel Marchi[b], Sophie Aligon[b], Antoine Bruguière[a], Chau Phi Dinh[a], Zahia Benbelkacem[a], Jean-Felix Dallery[b], Philippe Simoneau[b], Pascal Richomme[a*] and Thomas Guillemette[b*]

a Univ Angers, SONAS, SFR QUASAV, F-49000 Angers, France

b Univ Angers, Institut Agro, INRAE, IRHS, SFR QUASAV, 49070 Beaucouzé, France

* Pascal Richomme[a*] (pascal.richomme@univ-angers.fr) and

Thomas Guillemette[b*] (thomas.guillemette@univ-angers.fr)

Keywords: Natural products, UPR inhibitors, plant pathogenic fungi, crop protection

Abstract

Discovering new solutions for crop protection is a major challenge for the next decades due to the ecotoxicological impact of classical fungicides, the emergences of fungicide resistances and the consequences of climate change on pathogen distribution. Previous work on fungal mutants deficient in the Unfolded Protein Response (UPR) supported that targeting this pathway was a promising plant disease control strategy. In this study, we evaluated natural products targeting fungal IRE1 protein (UPR effector) and consequently reducing fungal resistance to plant defences. Developing an *in vitro* cell-based screening assay allowed the identification of seven potential IRE1 inhibitors with a focus on polyhydroxylated prenylated xanthones. Inhibition of *hac*1 mRNA splicing, which is mediated by IRE1, was then validated for the most active compound, namely γ-mangostin **3**. To study the mode of interaction between the binding site of IRE1 and active xanthones, molecular docking was also undertaken. Eventually, active xanthones applied at subtoxic doses induced significant reduction in necrosis size for plants inoculated with *Alternaria brassicicola* and *Botrytis cinerea*.

Introduction

From 1990s to present, global pesticide use has increased by 50% worldwide, reaching 4.2 million tons in 2019 [1]. This growing use of pesticides has a direct impact on environment, contaminating soils and water, reducing biodiversity and affecting human health (cancers, endocrine disruptors, neurological dysfunctions and respiratory disorders) [2]. As a consequence, around 750 active substances have been withdrawn from European market between 1993 and 2011 [3].

Among different crop threats, fungal diseases are the most devastating. Plant pathogenic fungi destroy a significant part of different food crops annually, up to 30% which would otherwise allow to feed 600 million people [4]. They also cause economical losses and pose a serious threat to food security [5]. Besides inorganic compounds *e.g.* sulfur or copper sulfate, which account for 42% of the total tonnage[6], fungicides are generally nitrogenous and/or sulfur organic compounds such as dithiocarbamates, benzimidazoles, diazoles, triazoles, diazines or morpholines. The potential toxicity of these pesticides for human and environment is associated with their molecular targets which are part of metabolic pathways, cellular respiration, tubulin polymerization or sterol biosynthesis [2,7].

In addition to this ecotoxicological impact, the permanent use of pesticides has to face severe limitations including the emergence of resistance in plant pathogens [8]. Moreover, global warming, which directly influences the dynamics and distribution of plant pathogens [5,9], reinforces the need for alternative crop protection [10], to ensure food security. To address this challenge, other pest and plant disease managements have been developed, such as biological control, which aims to inhibit pest or plant pathogens and/or to improve plant immunity through the effects of macro-organisms, beneficial micro-organisms, natural compounds, and semiochemicals. The use of biocontrol agents is growing at an estimated rate of 15 - 20% per year such that biocontrol substances represented 36.8 % of used agrochemical substances in 2018 [11].

Plants also naturally produce antimicrobial compounds such as phytoanticipins and phytoalexins as part of their defence system [12]. However, fungi have gradually acquired various protective mechanisms which allow them to overcome the effects of phytoalexins and thus continue their development in host tissues. To date, three main protective mechanisms have been identified in fungi: detoxification by efflux pumps[13,14] , inactivation by metabolism[13,14] and compensatory effects[15–18]. Previous works on the necrotrophic fungus *Alternaria brassicicola* have demonstrated the importance of compensatory effects[15] which include three different pathways, namely, Cell Wall Integrity (CWI)[15–17] , High Osmolarity Glycerol (HOG) pathway[15–17] and Unfolded Protein Response (UPR)[16,18,19] (Fig.1). It has also been shown that *A. brassicicola, Botrytis cinerea* and *Magnaporthe oryzae* mutants deficient in the UPR pathway exhibited a loss of virulence[18,20,21] associated with - for *A. brassicicola* - a higher susceptibility to glucosinolates (*e.g.* benzyl isothiocyanate **1**) and phytoalexins such as brassinin **2**[18]. These elements point to this pathway as an attractive target for the development of new antifungal strategies.

UPR pathway takes place in the endoplasmic reticulum (ER) of eukaryotic cells. It restores ER homeostasis, following accumulation of misfolded proteins, by inducing genes encoding chaperone proteins such as Binding immunoglobulin Protein (BiP) and foldases [22]. Different UPR effectors have been identified in eukaryotes. Metazoans have three effectors including the PKR-like ER Protein Kinase (PERK), the Activation Transcription Factor 6 (ATF6) and the Inositol-Requiring Enzyme 1 (IRE1a) [22]. In plants, the UPR pathway is mediated by two proteins orthologous to ATF6 and IRE1 (IRE1b) [23]. However, in fungi, the UPR pathway is governed by a single effector orthologous to IRE1 (IRE1p) [20] (Fig. S1).

IRE1 is a transmembrane protein with a luminal domain and a cytosolic domain which itself contains a kinase domain and a RNase one [22] (Fig. S2). The activation of the UPR pathway is initiated by an accumulation of misfolded proteins which leads to the dissociation of BiP from IRE1 to bind with misfolded proteins [22] (Fig. S1). This induces oligomerization of IRE1 followed by autophosphorylation and activation of the RNase domain. This domain promotes the splicing of the unique substrate of IRE1, the *hac*1 mRNA. This splicing allowed the removal of the transcriptional block of UPR pathways. Indeed, HAC1 protein is the major transcriptional regulator targeting genes related to the UPR pathway [22].

Therefore, we have been searching during this study for UPR inhibitors of natural origin targeting the activity of the IRE1 protein in plant pathogenic fungi for use as a biocontrol active substance. To this end, our initial experimental design focused on the establishment of a new *in vitro* cell-based screening assay, exploiting a reporter gene for the UPR pathway in *Saccharomyces cerevisiae*. The screening of 76 natural products was then completed, and, as a result, seven potential IRE1 inhibitors were identified (C, Fig.2). Subsequently, the impairment of *hac*1 mRNA splicing, mediated by IRE1, was validated for the most active compound namely γ-mangostin **3**. Eventually, *in planta* infections were monitored to assess the impact of UPR inhibitors against two phytopathogenic fungi, *A. brassicicola* and *B. cinerea*. Then, a molecular docking study of the inhibitors with IRE1 was carried out.

Materials and Methods

Materials

Dimethyl sulfoxide (DMSO, 99.7%) and dithiothreitol (DTT, 99%) were provided by Fisher bioreagents (New Jersey, USA), 3,5-diiodosalicylaldehyde (DISAl, 97%) was purchased from Acros Organics (New Jersey, USA).

All-natural compounds were present in the chemical library of the SONAS laboratory. Purity was controlled by HPLC-DAD-DEDL or by NMR. A minimum of 75% of purity was required for the screening test.

S. cerevisiae expressing GFP under control of HAC1 promoter

The splicing reporter construct was pRS305-hGFPh kindly provided by T. Aragon [24]. It was generated by replacing positions 1 to 648 of the HAC1 coding sequence in exon1 with the GFP ORF into the integrative plasmid pRS305. The intron, splice sites, and untranslated regions are identical to the *hac*1 mRNA. The plasmid was linearized by XcmI enzyme in LEU2 gene then genomically integrated into W303a yeast strain. Fluorescence experiments were conducted in synthetic media without Leucin (SD-Leu) prepared using low-fluorescence yeast nitrogen [25].

Screening Assay for IRE1 inhibition

The genetically modified reporter yeasts were maintained in SD-Leu culture medium and grown overnight at 30 °C with shaking (250 rpm) to a mid-log phase. Cell suspensions, diluted at 50.10^8 cells.L^{-1} in SD-Leu, were incubated with 10 µM control inhibitor (DISAl, **4**) or 10 µM each tested molecule in 1.4% DMSO during 30 min in a shaking incubator (30 °C-250 rpm). DTT was added to each tube at final concentration of 4 mM to induce the UPR response. 300 µL of treated cells were added in triplicate in each well of Falcon® 96-well Black/Clear Flat Bottom TC-treated Imaging Microplate, and the plate was placed in a Fluostar Omega microplate reader (BMG LABTECH) set at 30 °C with orbital shaking at 300 rpm for 3 hours. Both GFP Fluorescence, measured at 476 nm (ex)/512 nm (em) and cell growth, measured by OD 600 nm, were registered every 6 min. A triplicate was realized for each condition.

Fluorescence Increment Factor (FIF) was determined for each condition by a linear regression of the fluorescence data between 90 and 180 min, using R (3.4.4). FIF of molecules was normalized with FIF of positive control (4 mM, DTT) to obtain an activity percentage.

Isolation of RNA and RT-PCR analyses

5 mL of W303a yeast strain cells, diluted at 50.10^8 cells.L^{-1} were growth in synthetic dextrose medium at 30 °C, 250 rpm, with different concentrations of inhibitor during 30 min. DTT was added at the final concentration of 0.2 mM and incubated for 30 min to induce the UPR. Cells were collected by centrifugation, washed with cold water, then kept frozen at -80 °C until RNA extraction. Total RNA of treated yeast was extracted by Nucleospin® RNA Plus (Macherey-Nagel) according to manufacturer's protocols and quantified by nanodrop. Complementary DNA was synthesized from 5 µg of total RNA using the reverse-transcription system [50 mM Tris-HCl, 75 mM KCl, 10 mM DTT, 3 mM $MgCl_2$, 400 nM oligo(dT)15, 1 mM random hexamers, 0.5 mM dNTP, 200 units M-MLV reverse transcriptase, Promega]. The total volume was adjusted to 30 µL and the mixture was then incubated for 60 min at 42 °C. Aliquots

of 2 µL of the resulting first-strand cDNA were used for PCR amplification experiments with primers ScHAC1F3 5'- ACGACGCTTTTGTTGCTTCT-3' (forward) and ScHAC1R4 5'- AAATGAATTCAACCTGACTGC-3' (reverse). Amplification reactions were carried out in a total volume of 25 µL on a Bio-Rad R100TM thermocycler. Final concentrations of PCR components were as follows: PCR buffer without $MgCl_2$, 1.5 mM $MgCl_2$, 200 µM dNTPs, 0.4 µM of ScHAC1F3/ ScHAC1R4 each and 0.5 U of GoTaq DNA polymerase (Promega). After a pre-incubation step at 98 °C for 2 min, amplifications were performed for 35 cycles of denaturing at 95 °C for 30 s, annealing at 50 °C for 30 s, and extension at 72 °C for 45 s, followed by a final extension step of 7 min at 72 °C. Amplified DNA was analysed by 2% agarose gel electrophoresis using 0.5XTAE buffer.

Molecular docking

Molecular docking was performed on the cocrystal of cytosolic domain of murine IRE1 with MKC9989 inhibitor (PDB entry 4PL3, rcsb.org). To achieve molecular docking, MKC9989 was extracted of the binding site and the residue of LYS 907 was rectified. All implicit hydrogens were added using default setting of GOLD 5.6.3 (CCDC, Cambridge, UK). 4PL3 does not contain water molecules. After this modification protein was saved as a mol2 file.

Molecules were drawn (2D) by ChemDraw Professionnal 16.0 (PerkinElmer Informatics, Waltham, USA), and transferred in Ligandscout 4.4 (Inteligand, Vienna, Austria), to get their 3D structure follow-up by an energy minimization with the built-in MMFF94 function of LigandScout 4.4. The set of molecules was saved as a sdf file.

Rigid molecular docking procedure was conducted with GOLD 5.6.3, with protein 4PL3 and the set of molecules prepared like mentioned above. The binding site was defined in a 20 Å radius around the nitrogen atom of residue LYS 907. The CHEMPLP scoring function was used to rank the output poses. A maximal number of 10 poses were retained for each test molecule. Solutions of docking were extracted in pdb file to analyse interactions of ligand with the protein in LigandScout 4.4.

Fungal Growth curve monitoring

For inoculum preparation, conidia of *A. brassicicola* strain Abra 43 or *B. cinerea* strain B05.10 were collected from solid culture by adding water followed by gentle scraping of the agar plate. They were then counted in a Thoma's chamber and the conidial suspension was diluted to a final concentration of 10^6 conidia.mL^{-1} in water. A volume of 100 µL of conidia suspension was added in 890 µL of PDB medium and completed with 10 µL of the compound prepared in DMSO. Concentrations applied vary from 0.1 µM to 100 µM. 300 µL of treated conidia were added in triplicate in each well of Greiner® 96-well PS, F-Bottom, clear sterile microplate. Growth was monitored by nephelometric reader (NEPHELOstar Galaxy, BMG Labtech, Offenburg, Germany) at 25 °C, with orbital shaking 5 min before measurement for 33 h [26]. Turbidity was registered every 10 mins with a gain value of 75. Each well was measured during 0.1 s with a laser beam focus of 2.5 mm. A triplicate was realized for each condition. Area under the growth curve was determined by an Excel matrix developed in the lab and normalized by area of positive control (filamentous fungi + DMSO less compound) and PDB medium to obtain a growth percentage.

Infection assays

Plant infection assays were performed on leaves from 5-week-old plants (three to four leaves per plant) of *Brassica oleracea* var impala. 10 µL of molecules tested, prepared in DMSO, was added to 990 µL of *A. brassicicola* (Abra 43) or *B. cinerea* (B05.10) spore suspension (10^5 spores.mL^{-1} in a water with 10% of PDA medium). Final concentration of UPR inhibitors were as follows: against *A. brassicicola* 2 µM of **4**, 5 µM of **3**, 50 µM of **9** and 10 µM of **10**, and against *B. cinerea* 2,5 µM of **4** and 25 µM for the three prenylated xanthones **3**, **9** and **10**. 5 µL drops of inoculum was deposited on the left (without inhibitor) and right (with inhibitor) sides symmetrically from the central vein. The plants were then grown under saturating humidity, in dark for 48 h, then with 8 h light photoperiod for 3 days in control environment rooms (21-19 °C day and night temperature respectively). After this period, leaves were

photographed, and area of necrosis was measured with ImageJ. Three repetitions were performed for *A. brassicicola* and two for *B. cinerea*.

Statistical analysis

Area necrosis were analysed using Wilcoxon's Test with matched data or not, to compare areas necrosis with or without inhibitor (Table S2). Statistical analyses were performed using RStudio.

Results

IRE1 natural inhibitor screening assay

The monitoring of IRE1 activity was achieved through the use of the reporter gene system initially developed by Aragon *et al*. [24]. In this system, the first 648 nucleotides of the *hac*1 coding sequence in the first exon were replaced with those encoding the green fluorescent protein (GFP). The reporter mRNA was efficiently spliced following UPR induction, leading to an increase of fluorescence. In the presence of a UPR inhibitor, splicing was greatly reduced, and a decrease of fluorescence was observed (Fig. 2A). Dithiothreitol (DTT) was chosen as IRE1 elicitor [27].

To establish cell-based screening assay, four cell concentrations were tested (10, 30, 50 and 70.10^8 cells.L^{-1}) in combination with five DTT concentrations (2, 3, 4, 5 and 6 mM), in triplicate (Fig. S3). Fluorescence emission was monitored for 180 minutes. Fluorescence emission started after 60 minutes and appeared to linearly increase from 90 to 180 minutes (Fig. 2B). Fluorescence Increment Factor (FIF), corresponding to the regression coefficient between 90 and 180 minutes, was used as a criterion to compare each concentration pair. The combination of 50.10^8 cells.L^{-1} with 4 mM DTT was eventually selected (Fig. S3).

Dose response curves of four known inhibitors [28–30] were constructed using data from the cell-based assay. FIF were determined and normalized to express an activity percentage, denoted $\%_{act}$. When $\%_{act}$ reached 50%, the half maximal fluorescence inhibitory concentration, denoted IC_{50}, was determined. The most active inhibitor was 3,5-diiodosalicylaldehyde (DISAI) [29] **4** with an IC_{50} of 2.4 ± 0.2 µM (Fig. 2B), while the other three inhibitors tested (**A** 6-bromo-2-hydroxy-3-methoxybenzaldehyde. **B** 4µ8C. **C** 2-hydroxy-1-naphtaldehyde, Fig. S4) exhibited IC_{50} between 48 and 82 µM. Therefore, **4** was selected as the reference inhibitor compound, and the concentration of tested compounds was set to 10 µM. These IC_{50} obtained from the cell-based assay were higher than those obtained from enzymatic assay. For instance, IC_{50} of 6-bromo-2-hydroxy-3-methoxybenzaldehyde (Fig. S4A), in cell-based assay was 82.1 ± 0.1 µM versus 18 µM for enzymatic assay in yeast IRE1 [29]. This discrepancy between the activity on the enzyme and *in vivo* assay has already been observed [29,30], and could be related to the lipophilicity and bioavailability of compound in culture medium.

Then, a screening of 76 natural products exhibiting a large structural diversity (Table S1) was undertaken at 10 µM. To identify active compound, FIF of natural products were normalized in comparison with FIF of activation indicator to express a $\%_{act}$ (Fig. 2B). One compound is considered active when its $\%_{act}$ is below 80%.

This screening allowed to identify seven active compounds including: one caffeic acid cinnamyl ester **5** (71.9 ± 1.8 $\%_{act}$), one naphthoquinone [juglone **6** (47.9 ± 3.5 $\%_{act}$)], one isoquinoline alkaloid [oxostephanine **7** (79.8 ± 0.8 $\%_{act}$)]. The class of prenylated polyhydroxyxanthones was especially highlighted with α-mangostin **8** (66.8 ± 0.2 $\%_{act}$), 1,3,5-trihydroxy-2-prenylxanthone **9** (63.8 ± 4.2 $\%_{act}$), 1,3,5-trihydroxy-4-prenylxanthone **10** (70.4 ± 3.2 $\%_{act}$)] and γ-mangostin **3** (33.2 ± 8.0 $\%_{act}$). On the one hand, dose response evaluation (Fig. 2C) revealed **3** as the most effective compound with IC_{50} = 5.7 ± 0.3 µM *i.e.* close to the reference one. Surprisingly, **8** and **9** disclosed a partial inhibition. On the other hand, curcumin showed an activation level (171.3 ± 9.5 $\%_{act}$) higher than the positive control (DTT) (Table S1). Indeed, previous studies [31] already reported that curcumin targeted several MAP kinase pathways in fungi though it remained to be determined whether the impact on UPR was a direct effect on ER or a secondary effect related to other cellular disturbances [32].

Target validation: γ-mangostin (3) inhibited the *hac*1 mRNA splicing

To confirm that **3** effectively targeted IRE1, splicing inhibition of *hac*1 mRNA with (majority of splicing, denoted *hac*1^{s}) or without DTT (minority of splicing) was monitored in the presence of increasing concentrations and was compared to reference **4**. These experiments were performed with a *S. cerevisiae* wild type strain (W303a). In the presence of DTT, the ratio of unspliced *hac1* mRNA (*hac*1^{u}) clearly raised with increasing concentrations of **4** or **3** (Fig 3). At 25 µM (**4,** Fig. 3A) or 100 µM (**3**, Fig. 3B), a near complete inhibition of *hac1* mRNA splicing was observed. Therefore, the FIF reduction observed during the screening assay was directly correlated with IRE1 inhibition.

Molecular docking with RNase domain of IRE1

Docking studies were undertaken to identify the binding mode of xanthones within IRE1 active site. When compared with already described inhibitors of IRE1, the polyphenolic nature of active xanthones suggested that they would target the RNase domain of IRE1 (Fig. S2) unlike inhibitors containing nitrogen heterocycles target the kinase domain of IRE1 [33].

The cytosolic domain of IRE1 has already been crystallized and co-crystallized with ligands. However, no co-crystal of *S. cerevisiae* IRE1 contained a ligand in the RNase domain. Thus, a first approach was performed on a co-crystal of IRE1 (*Mus musculus*) with MKC9989[30] (Protein Data Bank, PDB 4PL3). Furthermore, amino acids at the binding site which interact with the ligand were well conserved between *M. musculus* and *S. cerevisiae* (Fig. 4A) since only Phe889 and Glu913 in *M. musculus* were replaced with amino acids of the same class in *S. cerevisiae,* namely Tyr1040 and Asp1064 respectively. Among three co-crystals of *M. musculus* IRE1, 4PL3 exhibits the best resolution (2.9 Å), along with a high reliability of the structure of the binding site. MKC9989 exhibit strong structural similarity with DISAI, due to the salicylaldehyde group which was described as an essential function for binding with IRE1 [34].

Moreover, 39 % of amino acids sequence of RNase domain of yeast IRE1 are shared with RNase domain of human IRE1 [35], and it has been demonstrated that yeast IRE1 cleaves a human mini-XBP1 RNA *in vitro*, and *vice versa* [29,36]. This showed the interchangeability of IRE1 between different organisms.

Therefore, the choice of this model based on IRE1 from *M.* musculus should be sufficiently consistent to decipher experimental data from cell-based assays and to establish the structure-activity relationships (SAR).

Redocking experiment was initially performed with MKC9989 : two π-staking interactions with His910 and Phe889, an hydrogen bond with Lys907 and a reciprocal hydrogen bond with Tyr892 were present as described in the literature [30] (Fig. 4B). The docking pose of **3** showed similar interactions with Phe889 and Tyr892 along with two new hydrogen bonds with Glu913 (Fig. 4C). **9** and **10** (Fig. S5) present similar docking poses than MKC9989 or **3** within the binding site and have interesting interactions with the same amino acids as described above for **3**. Eventually, **8** has only two π-staking interactions with Phe889 and hydrophobic contacts (Fig. S5), that can explain the inactivity of this xanthone.

UPR inhibitors applied at subtoxic doses reduced symptoms triggered by *A. brassicicola* and *B. cinerea*

The effect of UPR inhibitors against two necrotrophic fungi, namely *A. brassicicola* and *B. cinerea*, was studied *in planta*. To avoid false positives due to a direct biocide effect or fungistatic effect, subtoxic concentrations for xanthones **3**, **9**, **10** and DISAI **4** were defined. It was performed based on Middle Inhibition of Growth (MIG_{50}). **3** (MIG_{50} = 12.2 ± 0.2 µM), **10** (MIG_{50} = 41.3 ± 3.7 µM) and **4** (MIG_{50} = 5.3 ± 0.1 µM) inhibited the growth of *A. brassicicola* whilst only **4** (MIG_{50} = 6.2 ± 0.7µM) was efficient towards *B. cinerea* (Fig. 5A). Compound concentrations for *in planta* experiments were then adjusted to limit direct biocidal effects (less than 20% growth inhibition) (Fig. 5B).

At subtoxic concentration, it appeared that necrosis area for both necrotrophic fungi were significantly reduced in the presence of **3** (growth reduction of 43% for *A. brassicicola*, 81% for *B. cinerea*)**, 9** (82% for *A. brassicicola*, 70% for *B. cinerea*) and **10** (90% for *A. brassicicola*, 67% for *B. cinerea*). Surprisingly, DISAI **4** induced a slight reduction of necrosis area for *A. brassicicola* (38%) and did not impact the growth of *B. cinerea* in host tissues (Fig. 5C).

This low activity or inactivity is probably due to interactions between the aldehyde function (electrophilic) of **4** with nucleophilic groups from proteins. Alternatively, in consequence of the fungistatic action against two necrotrophic fungi, the concentrations applied *in planta* may be lower than the concentration necessary to act on IRE1.

Discussion

This work reports the development of a new strategy to control plant pathogenic fungi based on targeting the UPR pathway. To our knowledge, this signalling pathway has never been considered as a fungicide target in crop protection. Moreover, this mode of action is particularly original since the inhibitors are applied at doses that have little or no direct biocidal effect on epiphytic fungi inhabiting leaf surfaces. These inhibitors only weaken fungi that penetrate host tissue by making them more susceptible to the antimicrobial action of defence compounds. This plant disease control strategy is therefore based on a synergy of action between UPR inhibitors and plant antimicrobial compounds, allowing to target more specifically fungi initiating an infection process. This strategy seems particularly suitable for the control of necrotrophic fungi, such as *B. cinerea* or *A. brassicicola*, that are directly exposed to various host defence compounds (such as phytoalexins and/or phytoanticipins) during plant tissue colonization and that have usually developed several adaptive strategies to partially protect themselves against the toxic effects of these plant antimicrobial secondary metabolites and thus to achieve the infection process.

To go further, it now appears necessary to evaluate the efficiency of these inhibitors in controlling other major plant diseases, such as *Septoria* leaf blotch or downy mildew, both *in vitro* and in field crops. In parallel, it appears important to evaluate the impact of these compounds on the growth of beneficial fungi, such as *Trichoderma* species [37], that are used as biopesticides and biofertilizers. Ultimately, the use of these natural UPR inhibitors, alone or combined with other natural inhibitors of other compensatory pathways, such as CWI and HOG, is promising for both reducing the emergence of resistance (the doses applied have little or no direct effects on fungi) and limiting the use of synthetic pesticides.

As compared to *in vitro* cell-free screening assays, we consider that the cell-based screening assay used in this study has more physiological relevance, regarding the bioavailability of the candidate compounds and their cell penetration ability. Using this reporter gene assay, we showed that the decrease in fluorescence is directly correlated with the inhibition of the UPR pathway, identifiable by the accumulation of the unspliced *hac*1 mRNA. *Hac1* mRNA carries an atypical intron that prevents the synthesis of basic leucine zipper (bZIP)-type transcription factor Hac1p, which is the major UPR transcriptional regulator in fungi.

The modulation of UPR activity by xanthones or extract from mangosteen pericarp has already been described in human, but surprisingly xanthones were better known as UPR inducers [38,39]. Natural products identified in this study present a higher activity than known inhibitor such as 4μ8C[28] (Fig. S4). The binding mode to the active site should be different from that of the compounds described in the literature because the identified natural products do not have an aldehyde function able to covalently and reversibly bind to the amino residue of Lys907 (Fig 4). The current study showed that this covalent bond is not essential for the inhibition of IRE1. Moreover, the absence of this aldehyde function confers greater chemical and metabolic stability to this new family of IRE1 inhibitors. The structure-activity relationships study and molecular modelling suggested that the xanthene aromatic skeleton of xanthones is essential for the activity thanks to π-staking interactions with Phe889 and His910. The number and the position of the phenol functions also seem to be crucial for hydrogen bonds with the amino acids of the active site, specifically the phenol in position C3 with Tyr892 and the catechol function in C6-C7 with Glu913. Finally, the position and number of prenyl groups exhibiting hydrophobic

interactions also improve the inhibitory potential of the corresponding xanthones (Fig. S5). For a better understanding of SAR, pharmacomodulation study will be undertaken to increase activity of xanthones, considering physico-chemical parameters such as molecules solubility in growth media, lipophilicity and bioavailability with the aim of reducing inputs, supported by the French National scheme, Ecophyto.

Acknowledgments

The authors are very grateful to the South Province of New Caledonia, which has facilitated our field investigation.

We gratefully acknowledge Prof. Tomás Aragón for providing the plasmid pRS305-hGFPh.

Funding source

This research was conducted in the framework of the regional programme “Objectif Végétal, Research, Education and Innovation in Pays de la Loire”, supported by the French Region Pays de la Loire, Angers Loire Métropole and the European Regional Development Fund.

Note

The authors declare no conflict of interest.

References

(1) FAO. Pesticides Use, Pesticides Trade and Pesticides Indicators. Global, Regional and Country Trends, 1990–2019. *FAOSTAT Analytical Brief Series* **2021**, No. 29.

(2) Rani, L.; Thapa, K.; Kanojia, N.; Sharma, N.; Singh, S.; Grewal, A. S.; Srivastav, A. L.; Kaushal, J. An Extensive Review on the Consequences of Chemical Pesticides on Human Health and Environment. *J. Cleaner Prod.* **2021**, *283*, 124657. https://doi.org/10.1016/j.jclepro.2020.124657.

(3) Chapman, P. Is the Regulatory Regime for the Registration of Plant Protection Products in the EU Potentially Compromising Food Security? *Food Energy Secur* **2014**, *3* (1), 1–6. https://doi.org/10.1002/fes3.45.

(4) Avery, S. V.; Singleton, I.; Magan, N.; Goldman, G. H. The Fungal Threat to Global Food Security. *Fungal Biol* **2019**, *123* (8), 555–557. https://doi.org/10.1016/j.funbio.2019.03.006.

(5) Fisher, M. C.; Henk, Daniel. A.; Briggs, C. J.; Brownstein, J. S.; Madoff, L. C.; McCraw, S. L.; Gurr, S. J. Emerging Fungal Threats to Animal, Plant and Ecosystem Health. *Nature* **2012**, *484* (7393), 186–194. https://doi.org/10.1038/nature10947.

(6) Zhang, W. Global Pesticide Use: Profile, Trend, Cost / Benefit and More. **2018**, *8* (1), 1–27.

(7) Jampilek, J. Potential of Agricultural Fungicides for Antifungal Drug Discovery. *Expert Opin. Drug Discovery* **2016**, *11* (1), 1–9. https://doi.org/10.1517/17460441.2016.1110142.

(8) Fisher, M. C.; Hawkins, N. J.; Sanglard, D.; Gurr, S. J. Worldwide Emergence of Resistance to Antifungal Drugs Challenges Human Health and Food Security. *Science* **2018**, *360* (6390), 739–742. https://doi.org/10.1126/science.aap7999.

(9) Chaloner, T. M.; Gurr, S. J.; Bebber, D. P. Plant Pathogen Infection Risk Tracks Global Crop Yields under Climate Change. *Nat. Clim. Chang.* **2021**, *11* (8), 710–715. https://doi.org/10.1038/s41558-021-01104-8.

(10) Almeida, F.; Rodrigues, M. L.; Coelho, C. The Still Underestimated Problem of Fungal Diseases Worldwide. *Front. Microbiol.* **2019**, *10*, 214. https://doi.org/10.3389/fmicb.2019.00214.

(11) Robin, D. C.; Marchand, P. A. Evolution of the Biocontrol Active Substances in the Framework of the European Pesticide Regulation (EC) No. 1107/2009: Evolution of BCA within the Framework of Regulation (EC) No. 1107/2009. *Pest. Manag. Sci.* **2019**, *75* (4), 950–958. https://doi.org/10.1002/ps.5199.

(12) Tena, G.; Boudsocq, M.; Sheen, J. Protein Kinase Signaling Networks in Plant Innate Immunity. *Curr. Opin. Plant Biol.* **2011**, *14* (5), 519–529. https://doi.org/10.1016/j.pbi.2011.05.006.

(13) Westrick, N. M.; Smith, D. L.; Kabbage, M. Disarming the Host: Detoxification of Plant Defense Compounds during Fungal Necrotrophy. *Front. Plant Sci.* **2021**, *12*, 651716. https://doi.org/10.3389/fpls.2021.651716.

(14) Pedras, M. S. C.; Ahiahonu, P. W. K. Metabolism and Detoxification of Phytoalexins and Analogs by Phytopathogenic Fungi. *Phytochemistry* **2005**, *66* (4), 391–411. https://doi.org/10.1016/j.phytochem.2004.12.032.

(15) Joubert, A.; Bataille-Simoneau, N.; Campion, C.; Guillemette, T.; Hudhomme, P.; Iacomi-Vasilescu, B.; Leroy, T.; Pochon, S.; Poupard, P.; Simoneau, P. Cell Wall Integrity and High Osmolarity Glycerol Pathways Are Required for Adaptation of *Alternaria Brassicicola* to Cell Wall Stress Caused by Brassicaceous Indolic Phytoalexins: Camalexin Activation of HOG and CWI Pathways. *Cell. Microbiol.* **2011**, *13* (1), 62–80. https://doi.org/10.1111/j.1462-5822.2010.01520.x.

(16) N'Guyen, G. Q.; Raulo, R.; Porquier, A.; Iacomi, B.; Pelletier, S.; Renou, J.-P.; Bataillé-Simoneau, N.; Campion, C.; Hamon, B.; Kwasiborski, A.; Colou, J.; Benamar, A.; Hudhomme, P.; Macherel, D.; Simoneau, P.; Guillemette, T. Responses of the Necrotrophic Fungus *Alternaria Brassisicola* to the Indolic Phytoalexin Brassinin. *Front. Plant Sci.* **2021**, *11*, 611643. https://doi.org/10.3389/fpls.2020.611643.

(17) Zhang, X.; Wang, Z.; Jiang, C.; Xu, J.-R. Regulation of Biotic Interactions and Responses to Abiotic Stresses by MAP Kinase Pathways in Plant Pathogenic Fungi. *Stress Biol.* **2021**, *1* (1), 5. https://doi.org/10.1007/s44154-021-00004-3.

(18) Joubert, A.; Simoneau, P.; Campion, C.; Bataillé-Simoneau, N.; Iacomi-Vasilescu, B.; Poupard, P.; François, J. M.; Georgeault, S.; Sellier, E.; Guillemette, T. Impact of the Unfolded Protein Response on the Pathogenicity of the Necrotrophic Fungus *Alternaria Brassicicola* : Impact of the UPR on *Alternaria Brassicicola* Virulence. *Mol. Microbiol.* **2011**, *79* (5), 1305–1324. https://doi.org/10.1111/j.1365-2958.2010.07522.x.

(19) Guillemette, T.; Calmes, B.; Simoneau, P. Impact of the UPR on the Virulence of the Plant Fungal Pathogen *A. Brassicicola*. *Virulence* **2014**, *5* (2), 357–364. https://doi.org/10.4161/viru.26772.

(20) Krishnan, K.; Askew, D. S. Endoplasmic Reticulum Stress and Fungal Pathogenesis. *Fungal Biol. Rev.* **2014**, *28* (2–3), 29–35. https://doi.org/10.1016/j.fbr.2014.07.001.
(21) Zhang, H.; Li, Y.; Dickman, M. B.; Wang, Z. Cytoprotective Co-Chaperone BcBAG1 Is a Component for Fungal Development, Virulence, and Unfolded Protein Response (UPR) of *Botrytis Cinerea*. *Front. Microbiol.* **2019**, *10*, 685. https://doi.org/10.3389/fmicb.2019.00685.
(22) Adams, C. J.; Kopp, M. C.; Larburu, N.; Nowak, P. R.; Ali, M. M. U. Structure and Molecular Mechanism of ER Stress Signaling by the Unfolded Protein Response Signal Activator IRE1. *Front. Mol. Biosci.* **2019**, *6*, 11. https://doi.org/10.3389/fmolb.2019.00011.
(23) Wan, S.; Jiang, L. Endoplasmic Reticulum (ER) Stress and the Unfolded Protein Response (UPR) in Plants. *Protoplasma* **2016**, *253* (3), 753–764. https://doi.org/10.1007/s00709-015-0842-1.
(24) Aragón, T.; van Anken, E.; Pincus, D.; Serafimova, I. M.; Korennykh, A. V.; Rubio, C. A.; Walter, P. Messenger RNA Targeting to Endoplasmic Reticulum Stress Signalling Sites. *Nature* **2009**, *457* (7230), 736–740. https://doi.org/10.1038/nature07641.
(25) Sheff, M. A.; Thorn, K. S. Optimized Cassettes for Fluorescent Protein Tagging in *Saccharomyces Cerevisiae*. *Yeast* **2004**, *21* (8), 661–670. https://doi.org/10.1002/yea.1130.
(26) Joubert, A.; Calmes, B.; Berruyer, R.; Pihet, M.; Bouchara, J.-P.; Simoneau, P.; Guillemette, T. Laser Nephelometry Applied in an Automated Microplate System to Study Filamentous Fungus Growth. *BioTechniques* **2010**, *48* (5), 399–404. https://doi.org/10.2144/000113399.
(27) Mizuno, T.; Nakamura, M.; Irie, K. Induction of Ptp2 and Cmp2 Protein Phosphatases Is Crucial for the Adaptive Response to ER Stress in *Saccharomyces Cerevisiae*. *Sci Rep* **2018**, *8* (1), 13078. https://doi.org/10.1038/s41598-018-31413-6.
(28) Cross, B. C. S.; Bond, P. J.; Sadowski, P. G.; Jha, B. K.; Zak, J.; Goodman, J. M.; Silverman, R. H.; Neubert, T. A.; Baxendale, I. R.; Ron, D.; Harding, H. P. The Molecular Basis for Selective Inhibition of Unconventional MRNA Splicing by an IRE1-Binding Small Molecule. *Proc. Natl. Acad. Sci. U.S.A.* **2012**, *109* (15), E869–E878. https://doi.org/10.1073/pnas.1115623109.
(29) Volkmann, K.; Lucas, J. L.; Vuga, D.; Wang, X.; Brumm, D.; Stiles, C.; Kriebel, D.; Der-Sarkissian, A.; Krishnan, K.; Schweitzer, C.; Liu, Z.; Malyankar, U. M.; Chiovitti, D.; Canny, M.; Durocher, D.; Sicheri, F.; Patterson, J. B. Potent and Selective Inhibitors of the Inositol-Requiring Enzyme 1 Endoribonuclease. *J. Biol. Chem.* **2011**, *286* (14), 12743–12755. https://doi.org/10.1074/jbc.M110.199737.
(30) Sanches, M.; Duffy, N. M.; Talukdar, M.; Thevakumaran, N.; Chiovitti, D.; Canny, M. D.; Lee, K.; Kurinov, I.; Uehling, D.; Al-awar, R.; Poda, G.; Prakesch, M.; Wilson, B.; Tam, V.; Schweitzer, C.; Toro, A.; Lucas, J. L.; Vuga, D.; Lehmann, L.; Durocher, D.; Zeng, Q.; Patterson, J. B.; Sicheri, F. Structure and Mechanism of Action of the Hydroxy–Aryl–Aldehyde Class of IRE1 Endoribonuclease Inhibitors. *Nat. Commun.* **2014**, *5* (1), 4202. https://doi.org/10.1038/ncomms5202.
(31) Hua, C.; Kai, K.; Wang, X.; Shi, W.; Zhang, D.; Liu, Y. Curcumin Inhibits Gray Mold Development in Kiwifruit by Targeting Mitogen-Activated Protein Kinase (MAPK) Cascades in *Botrytis Cinerea*. *Postharvest Biol. and Technol.* **2019**, *151*, 152–159. https://doi.org/10.1016/j.postharvbio.2019.02.006.
(32) Scrimale, T.; Didone, L.; de Mesy Bentley, K. L.; Krysan, D. J. The Unfolded Protein Response Is Induced by the Cell Wall Integrity Mitogen-Activated Protein Kinase Signaling Cascade and Is Required for Cell Wall Integrity in *Saccharomyces Cerevisiae*. *Mol. Biol. Cell* **2009**, *20* (1), 164–175. https://doi.org/10.1091/mbc.e08-08-0809.
(33) Ferri, E.; Le Thomas, A.; Wallweber, H. A.; Day, E. S.; Walters, B. T.; Kaufman, S. E.; Braun, M.-G.; Clark, K. R.; Beresini, M. H.; Mortara, K.; Chen, Y.-C. A.; Canter, B.; Phung, W.; Liu, P. S.; Lammens, A.; Ashkenazi, A.; Rudolph, J.; Wang, W. Activation of the IRE1 RNase through Remodeling of the Kinase Front Pocket by ATP-Competitive Ligands. *Nat. Commun.* **2020**, *11* (1), 6387. https://doi.org/10.1038/s41467-020-19974-5.
(34) Tomasio, S. M.; Harding, H. P.; Ron, D.; Cross, B. C. S.; Bond, P. J. Selective Inhibition of the Unfolded Protein Response: Targeting Catalytic Sites for Schiff Base Modification. *Mol. BioSyst.* **2013**, *9* (10), 2408. https://doi.org/10.1039/c3mb70234k.
(35) Tirasophon, W.; Welihinda, A. A.; Kaufman, R. J. A Stress Response Pathway from the Endoplasmic Reticulum to the Nucleus Requires a Novel Bifunctional Protein Kinase/Endoribonuclease (Ire1p) in Mammalian Cells. *Genes Dev.* **1998**, *12*, 1812–1824. https://doi.org/10.1101/gad.12.12.1812.
(36) Lee, K. P. K.; Dey, M.; Neculai, D.; Cao, C.; Dever, T. E.; Sicheri, F. Structure of the Dual Enzyme Ire1 Reveals the Basis for Catalysis and Regulation in Nonconventional RNA Splicing. *Cell* **2008**, *132*, 89–100. https://doi.org/10.1016/j.cell.2007.10.057.

(37) Poveda, J. *Trichoderma* as Biocontrol Agent against Pests: New Uses for a Mycoparasite. *Biol. Control* **2021**, *159*, 104634. https://doi.org/10.1016/j.biocontrol.2021.104634.
(38) Ovalle-Magallanes, B.; Eugenio-Pérez, D.; Pedraza-Chaverri, J. Medicinal Properties of Mangosteen (*Garcinia Mangostana* L.): A Comprehensive Update. *Food and Chem. Toxicol.* **2017**, *109*, 102–122. https://doi.org/10.1016/j.fct.2017.08.021.
(39) Li, G.; Petiwala, S. M.; Pierce, D. R.; Nonn, L.; Johnson, J. J. Selective Modulation of Endoplasmic Reticulum Stress Markers in Prostate Cancer Cells by a Standardized Mangosteen Fruit Extract. *PLoS ONE* **2013**, *8* (12), e81572. https://doi.org/10.1371/journal.pone.0081572.
(40) Vela-Corcía, D.; Aditya Srivastava, D.; Dafa-Berger, A.; Rotem, N.; Barda, O.; Levy, M. MFS Transporter from *Botrytis Cinerea* Provides Tolerance to Glucosinolate-Breakdown Products and Is Required for Pathogenicity. *Nat. Commun.* **2019**, *10* (1), 2886. https://doi.org/10.1038/s41467-019-10860-3.

Figures and Tables

Figure 1. Protective mechanisms of necrotrophic fungus during infection of host plant such as cultivated *Brassicaceae*.

(1) Fungal infection in host cells induces a Ca^{2+} influx which triggers host plant signalling pathways. This leads (2) to the production of defence compounds (peptides, specialized metabolites…) and enzymes[12]. (3) In *Brassicaceae*, such compounds like benzyl isothiocyanate **1** target mitochondria whilst generating reactive oxygen species (ROS). (4) Then production of phytoalexins such as brassinin **2** not only exhibits similar effects than **1** but has an impact on lipid homeostasis and belatedly on granular endoplasmic reticulum (ER) homeostasis[16]. (5) These different stresses trigger in fungal cells the activation of compensatory responses including Cell Wall Integrity (CWI), High-osmolarity glycerol (HOG), and Unfolded Protein Response (UPR)[16,17]. (6) Outputs of activated pathways contribute to protect the fungal cell against the effects of antimicrobial plant metabolites. (7) In parallel, fungi (*e.g. A. brassicicola* or *B. cinerea*) show another protective mechanism: detoxification, that may be performed by transporter-mediated efflux such as Major Facilitator Superfamily (MFS), and/or metabolism of defence compounds to less toxic derivatives[13,40]. (8) These protective mechanisms are required for full virulence.

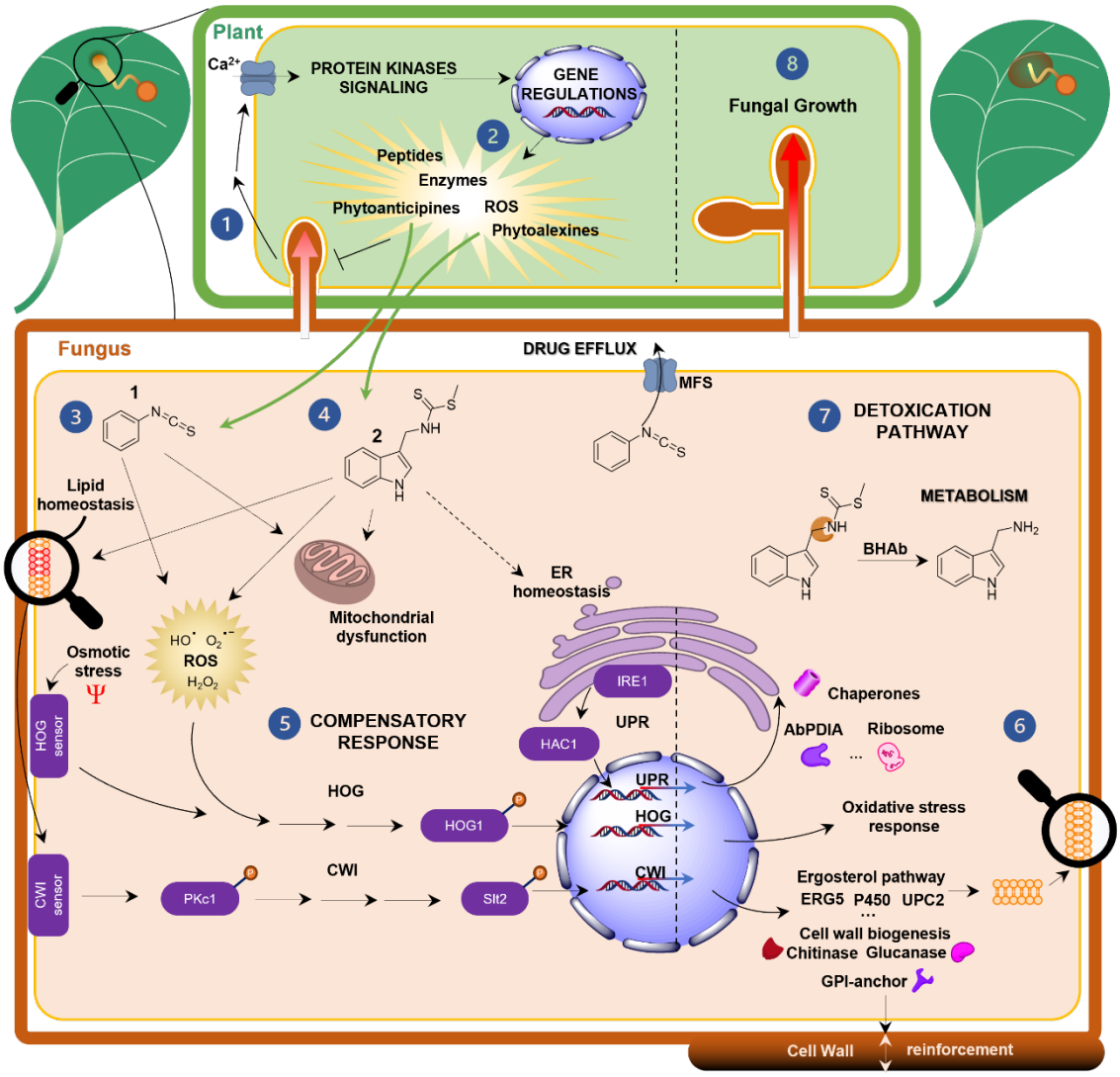

Figure 2. IRE1 inhibitors screening assay.
A UPR pathway description in the transformed *S. cerevisiae*. UPR is activated by DTT treatment (4 mM). Upon ER stress, according to the allosteric model, Binding immunoglobulin Proteins (BiP) dissociate from IRE1 which is subsequently oligomerized, then autophosphorylated to eventually activate the RNase domain (in green). This allows splicing of specific substrate *hac*1 mRNA containing the coding sequence for GFP. In the presence of an IRE1 inhibitor, splicing and fluorescence emission are reduced. **B** Emission fluorescence curves with different concentrations of DISAI **4**. The evaluation of activity percentage was expressed by the normalization of Fluorescence Increment Factors (FIF) between 90 min and 180 min with respect to the FIF of activation control (4 mM DTT). Finally, IC_{50} of DISAI was determined. **C** Structures and dose-response experiments of cinnamyl caffeate **5**, juglone **6**, oxostephanine **7**, α-mangostin **8**, γ-mangostin **3**, 1,3,5-trihydroxy-2-prenylxanthone **9** and 1,3,5-trihydroxy-4-prenylxanthone **10**. IC_{50} was determined when $\%_{act}$ reached 50%. IC_{50} values represent mean ± SD of three dose-response experiment.

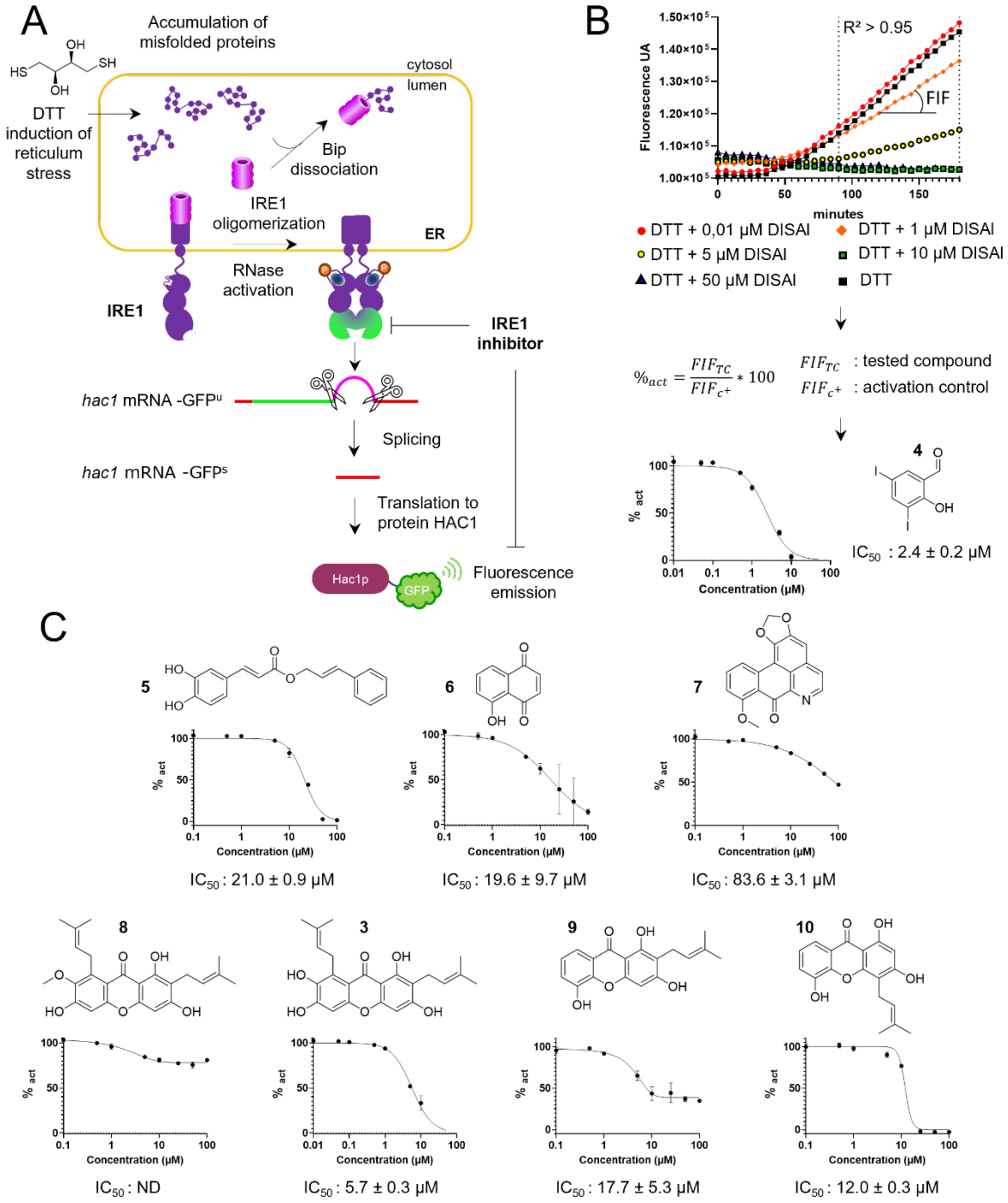

Figure 3. Inhibition of *hac1* mRNA splicing in *S. cerevisiae* cells (WT) exposed to increasing amounts of DISAl **4 A** or γ-mangostin **3 B**. Cell suspension at 50.10^8 cells.L^{-1} were incubated with different concentrations of inhibitor during 30 min. Then DTT was added at the final concentration of 4 mM during 30 min to induce UPR pathway.

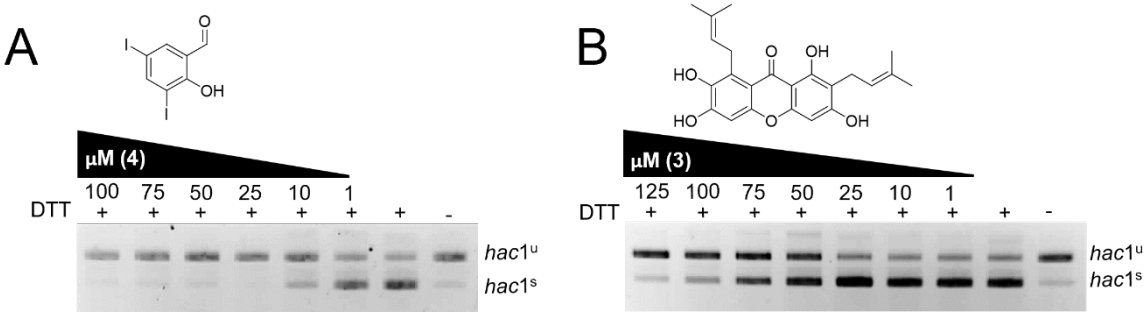

Figure 4. Molecular docking of the RNase domain of IRE1 (4PL3).
A Protein sequence alignment of the binding site of *M. musculus*, *S. cerevisiae*, *A. brassicicola* and *B. cinerea.* Identified amino acids are those interacting with MKC9989 in IRE1 binding site from *M. musculus* (in green similarities, in red differences between *M. musculus* sequence and the three other sequences). **B** Cytosolic domain of IRE1 monomers docked with MKC9989. On the right, main interactions between MKC9989 and the binding site of IRE1. **C** Docking pose and the main interactions between γ-mangostin **3** and binding site of IRE1.

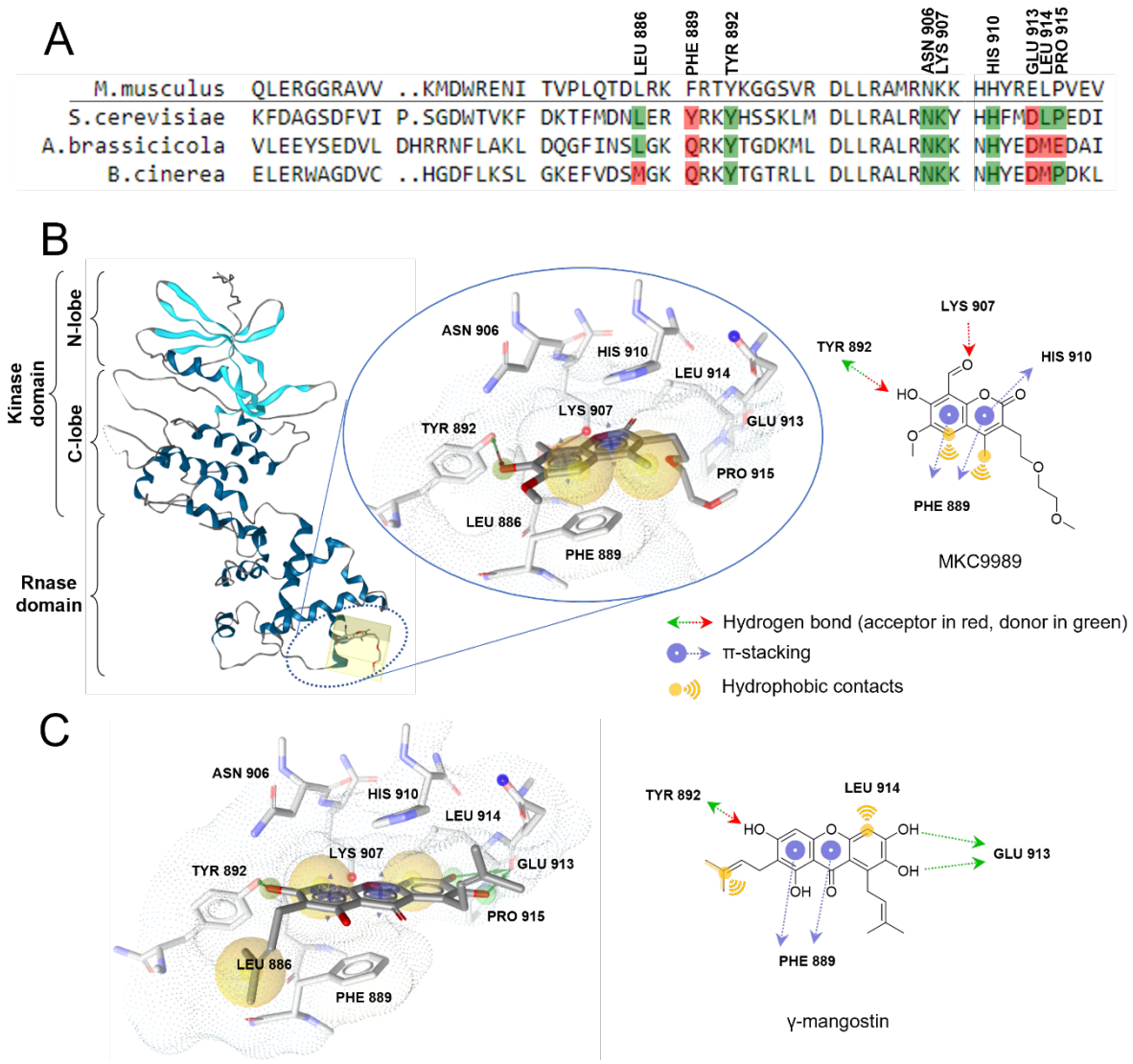

Figure 5. Plant infection assays.
A MIG_{50} determination of γ-mangostin **3**, 1,3,5-trihydroxy-2-prenylxanthone **9**, 1,3,5-trihydroxy-4-prenylxanthone **10** and DISAl **4** for two necrotrophic pathogens *A. brassicicola* and *B. cinerea.* MIG_{50} values represent mean ± SD of three dose-response experiment.
B Subtoxic concentrations of UPR inhibitors applied to the plants **C** Necrosis area of both plant pathogens *A. brassicicola* and *B. cinerea.* The untreated fungal inoculum was applied on the left part of the central vein (**a**) and the fungus exposed to the inhibitor was inoculated on the right part (**b**) of the same leaf.
*, **, *** Indicated significant difference of necrosis area with inhibitors against without with p-value < 0.05, <0.01, <0.001 respectively, obtained by Wilcoxon test with paired data
°, °°, °°° Indicated significant difference of necrosis area with inhibitors against without with p-value < 0.05, <0.01, <0.001 respectively , obtained by Wilcoxon test with unpaired data

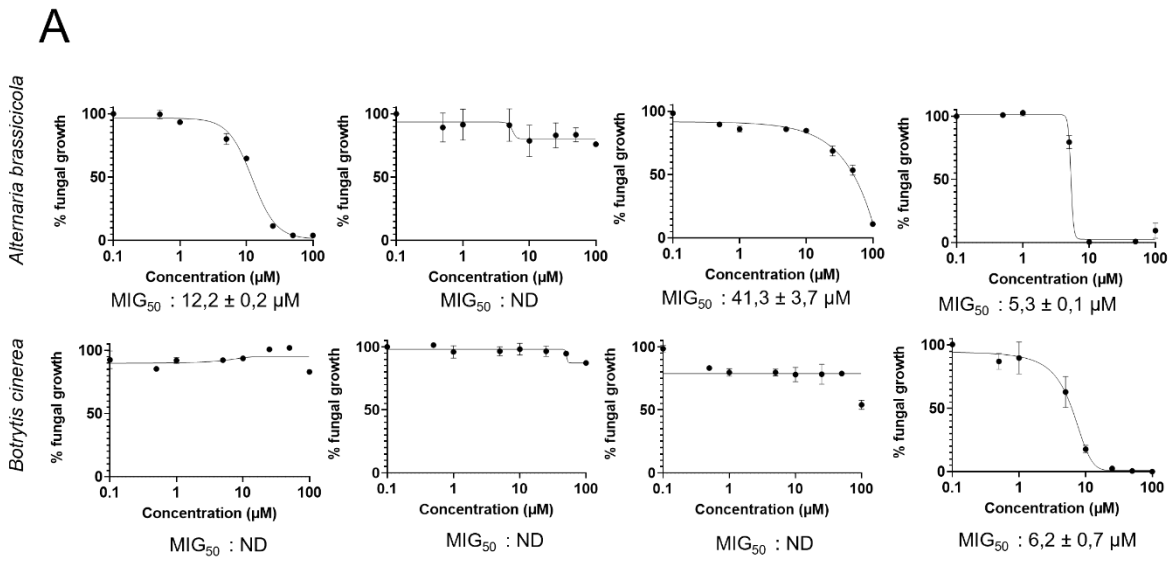

B

Concentration applied *in planta*

	3	9	10	4
A. brassicicola	5 µM	50 µM	10 µM	2 µM
B. cinerea	25 µM	25 µM	25 µM	2,5 µM